Asia Pac. J. Math. 2024 **11**:105

CONSTRUCTION OF RLUF-TYPE COPULA GENERATED BY RÜSCHENDORF METHOD TO MODEL TIME-VARYING DEPENDENCY FOR DENGUE R_{eff}, PRECIPITATION AND TEMPERATURE

JOE VINCENT B. DELUAO[1,*], MILBURN O. MACALOS[2], JAYROLD P. ARCEDE[2]

[1]Department of Mathematics, University of Southeastern Philippines, Philippines

[2]Department of Mathematics, Caraga State University, Philippines

[*]Corresponding author: joe.deluao@usep.edu.ph

Received Oct. 10, 2024

Abstract. In this study, an RLUF-type copula was constructed using the Rüschendorf method to model the dependence structure between climatic variables: daily precipitation and temperature; and Dengue's Effective Reproductive number, R_{eff}. We derived key dependence measures, including Kendall's tau, Spearman's rho, and upper-lower tail dependences. Using the Inference function for margins, we found that R_{eff} follows a three-parameter logistic distribution, daily precipitation aligns with the three-parameter Generalized Pareto distribution, and temperature fits the Burr distribution. These marginal distributions were integrated into the RLUF-type copula, which demonstrated superior predictive performance compared to traditional copulas, such as Clayton, Gumbel, and Frank, as indicated by lower AIC and BIC values. We also derived a closed-form joint cumulative distribution function (CDF) based on Sklar's theorem for pairings of R_{eff} with temperature and precipitation. Additionally, a time-varying version of the RLUF-type copula was developed by estimating the dependence parameter θ through a rolling time-window approach using the ARIMA routine, which further improved the prediction accuracy. This time-varying copula was then applied to predict the probability of a decrease in dengue transmission, given changes in climatic conditions.

2020 Mathematics Subject Classification. 62H05; 60E05.

Key words and phrases. RLUF copula; Ruschendorf method; time-varying copula; conditional probability models; ARIMA.

1. Introduction

Dengue fever continues to pose a critical public health challenge in the Philippines, a situation exacerbated by the country's warm and humid climate, which creates ideal breeding conditions for the *Aedes aegypti* mosquito, the primary vector of the dengue virus. Recent epidemiological data highlight

DOI: 10.28924/APJM/11-105

a 30% rise in dengue cases as of June 29, 2024, totaling 90,119 cases and 233 deaths, which marks a 19% increase compared to the same period in 2023. Particularly alarming is the Caraga Region, where cases have surged by 144%, reaching epidemic levels with 7,122 cases and 39 deaths reported from January 1 to August 17, 2024 [1,27]. These figures illustrate the intensifying strain on public health resources and underscore the urgency of identifying effective mitigation strategies.

Research increasingly demonstrated that dengue transmission is intricately linked to climatic variables, particularly to precipitation and temperature. Precipitation, by creating stagnant water bodies, facilitates mosquito breeding, leading to increased mosquito populations and consequently, higher transmission rates [6,23]. Temperature also plays a critical role by accelerating mosquito life cycles and reducing the incubation period of the virus, thereby enhancing the transmission efficiency [5,35]. Studies have consistently shown that as the temperature increases, dengue incidence also tends to increase [6,16,21,30,37–39]. Moreover, the interaction between high temperatures and heavy rainfall compounds this effect, highlighting the complex and non-linear relationships between climate and disease spread [6,16,37]. Understanding these dependencies is essential for developing robust forecasting and intervention strategies.

Traditionally, the prediction of dengue incidence has relied on statistical models such as regression analysis and time series models [22,25], which often assume linear relationships and focus on marginal effects. These models, however, may not adequately capture the non-linear and joint dependencies between climatic factors. For example, the relationship between temperature and precipitation is likely to be highly complex, and an isolated focus on either factor may not reflect their combined impact on dengue transmission. Moreover, machine learning approaches have gained popularity in recent years for spatial modeling of dengue spread [15,19,40]. While these models can achieve high predictive accuracy, they often function as "black boxes," offering little interpretability regarding the specific interactions between climatic factors and disease outcomes. Additionally, machine learning models may suffer from overfitting, especially in the presence of limited or noisy epidemiological data, and they typically do not account for the temporal lag effects that are crucial in understanding the delayed impact of climatic conditions on dengue outbreaks.

To address these limitations, copula models offer a promising alternative by providing a flexible framework for modeling complex dependencies between multiple variables, independent of their marginal distributions. Introduced by Sklar in 1959, copulas have been widely adopted in fields such as finance and insurance, following the pioneering work of Embrechts and co-authors in 1999 [13,28]. More recently, they have found applications in diverse areas, including energy, forestry, and environmental sciences [4], where understanding the dependencies between variables is critical for accurate prediction and risk assessment.

Copula models are particularly advantageous in the context of dengue transmission, for several reasons. First, they allow for the modeling of nonlinear dependencies, capturing the intricate relationships between temperature, precipitation, and dengue incidence more effectively than traditional linear models. For instance, copulas can model situations in which the combined effects of temperature and precipitation lead to a disproportionate increase in dengue transmission, effects that would be missed in a linear model. Second, copulas enable the use of different marginal distributions for each variable, which allows for greater flexibility when modeling climatic variables that may follow different statistical distributions. This is particularly useful when dealing with variables such as precipitation, which often exhibits skewed distributions, while temperature may follow a more symmetric pattern [18,29].

In addition, copulas can be extended to incorporate time-varying structures [9], which are critical for modeling the dynamic relationships between climatic factors and dengue transmission over time. Climatic variables such as rainfall may influence dengue incidence with a temporal lag, and dengue cases often rise several weeks after periods of heavy rainfall owing to the mosquito breeding cycle [8]. Time-varying copulas allow us to model these lead-lag relationships, capturing how the dependence between climatic factors and dengue changes dynamically over time. Finally, copulas are uniquely suited for capturing tail dependence [10] and the tendency of extreme climatic events (e.g., an unusually hot and wet season) to coincide with extreme dengue outbreaks. This feature makes copulas particularly valuable for predicting high-risk scenarios and providing better early warning for public health interventions.

While many existing dengue prediction models have focused on marginal effects or advanced machine learning techniques, a few studies have applied copula models to investigate the joint dependence of precipitation and temperature [3,7,11,17,31,32,41,42]. To date, there have been no copula studies related to dengue transmission. This represents a significant gap in the literature, and addressing this gap is essential for improving dengue forecasting models.

This study investigated the dependence structure between dengue spread and climatic factors, such as precipitation and temperature, using copula models to fill this gap. Specifically, we construct a novel RLUF copula based on the Rüschendorf method and compare its performance in modeling these dependencies to that of existing Archimedean copulas by employing the inference function for margins (IFM) method. In addition, we will extend our models to incorporate time-varying copulas, allowing us to capture the dynamic and evolving relationships between dengue spread and climatic factors. By modeling both the nonlinear interactions and the temporal lags between climate variables and dengue incidence, our approach aims to provide more accurate and interpretable insights into the drivers of dengue outbreaks.

2. Materials and Methods

2.1. **Data Collection.** Data on daily dengue cases in the Caraga Region, Philippines, from January 2015 to December 2020, were used to compute the dengue effective reproductive number, R_{eff}, using the SIR-UV model in [33]. Daily temperature (°C) and precipitation (mm) data for the same period were sourced from the NASA POWER Data Viewer https://power.larc.nasa.gov/data-access-viewer/. These variables form the basis for modeling the dependency structure.

2.2. **Copula Framework.** In this section, we describe the construction of a copula and how it will be applied to model the dependency of the climatic factors and the spread of dengue.

A bivariate copula C is a function of two variables U_1 and U_2, each defined in $[0,1]$ such that:

(1) The range of the copula $C(u_1,u_2)$ is in the unit interval $[0,1]$;
(2) $C(u_1,u_2)=0$ if any $u_i=0$ for $i=1,2$;
(3) $C(1,u_2)=u_2$ and $C(u_1,1)=u_1$.

Sklar's theorem shows the relationship between a bivariate copula function C and a bivariate distribution. Let X_1 and X_2 be two random variables and let $F(x_1,x_2)=P(X_1\le x_1, X_2\le x_2)$ be the joint distribution function with marginals $F(x_1)$ and $F(x_2)$. Then, there exists a bivariate copula function such that

$$F(x_1,x_2)=C(F(x_1),F(x_2)).$$

Therefore, define $u_i=F(x_i)$,

$$C(u_1,u_2)=F(x_1,x_2).$$

Several copula functions can be used to model the relationship between rainfall and temperature. The most common include the Gaussian copula, Student's t-copula, Clayton copula, and the Gumbel copula. The choice of copula function depends on the nature of the relationship between rainfall and temperature and the available data. However, in this paper, we will construct such a function through Rüschendord method [36], while verifying it to be a copula, thanks to a result by [34] and compared it to Clayton, Ali-Mikhail-Haq (AMH), Frank, Gumbel, Joe, Farlie-Gumbel-Morgenstern (FGM) copulas.

Because we only need a two-dimensional construction, we follow the construction presented in [26]. However, the procedure can be applied to a multivariate case, see [2]. The procedure starts with an arbitrary real integrable function $f(x,y)$ on $[0,1]^2$ and compute its marginals (i) $f_1(x)=\int_0^1 f(x,y)dy$, (ii) $f_2(y)=\int_0^1 f(x,y)dx$ and (iii) $A=\int_0^1\int_0^1 f(x,y)dydx$. By reassembling, $f^1(x,y)=f(x,y)-f_1(x)-f_2(y)+A$, we set $c(x,y)=1+\theta f^1(x,y)$, so that we have constructed the function

$$C(u,v)=uv+\theta\int_0^u\int_0^v f^1(x,y)dydx \tag{1}$$

to be verified as copula through following result.

Theorem 2.1. *Let f and g be two non-zero absolutely continuous functions defined on $[0,1]$ such that $f(0) = f(1) = g(0) = g(1)$. Let C_θ be a function defined on $[0,1]^2$ by $C_{theta}(uv) = uv + \theta f(u)g(v)$, with $\theta \in \mathbb{R}$. Then, C_θ is a copula if and only if*

$$-\frac{1}{\max\{\alpha\gamma, \beta\delta\}} \leq \theta \leq -\frac{1}{\min\{\alpha\delta, \beta\gamma\}}$$

where $\alpha = \inf\{f'(u) : u \in A\} < 0,\ \beta = \sup\{f'(u) : u \in A\} > 0, \gamma = \inf\{g'(v) : v \in B\} < 0$, and $\delta = \sup\{g'(v) : v \in B\} > 0$, with $A = \{u \in [0,1] : f'(u)$ exists$\}$ and $B = \{v \in [0,1] : g'(v)$ exists$\}$.

Theorem 2.1 specifies the necessary and sufficient requirements for a bivariate copula to be characterized by two real functions, f and g. It asserts that the function C_θ is a valid copula if and only if the functions f and g are absolutely continuous on [0,1] and meet certain derivative criteria. The copula C_θ is coined in literature as the RLUF copula [43].

2.3. **Model Fitting and Validation.** In this study, model fitting for the copula was conducted using the inference function for margins (IFM), a two-step procedure. First, the marginal distribution of each variable was estimated independently. This involved selecting the appropriate univariate distribution for each variable based on statistical criteria such as the chi-square test, Mean Squared Error (MSE), Akaike Information Criterion (AIC), and Bayesian Information Criterion (BIC). The process begins by fitting the observed data to a candidate univariate distribution, where the parameters of the chosen distribution are estimated by minimizing the MSE:

$$MSE = \frac{1}{n-m}\sum_{i=1}^{n}(O_i - E_i)^2$$

where n represents the number of observations, m the number of fitted parameters, O_i the observed value, and E_i the expected value. If the chi-square test statistic is less than the critical value, the null hypothesis (H_0) is accepted, indicating that the selected distribution provides a satisfactory fit to the data. Otherwise, alternative distributions were tested iteratively until the best fit was determined, which was the one with the lowest MSE, AIC, and BIC. Once the best-fitting marginal distributions are identified, the second step involves selecting and fitting the copula model. The parameters of the selected copula were estimated by fitting the model to the data using methods such as the maximum likelihood estimation (MLE). The copula's goodness of fit was again assessed using statistical criteria (MSE, AIC, and BIC) to ensure that the model accurately captured the dependencies between the variables. For each pair of variables, the copula with the smallest MSE, AIC, and BIC values was considered to be the best-fitting model. For example, in fitting the copula for the relationship between Dengue's effective reproductive number (R_{eff}) and precipitation, the RLUF copula outperformed other models such as the Clayton and Frank copulas. The final copula minimized the MSE and yielded lower AIC and BIC values, indicating a superior fit to the observed data.

Time-varying copulas were introduced by estimating copula parameter θ_t using a rolling time window approach. This method allows the copula parameter to vary over time, thus capturing the evolving dependencies between variables. The estimation of θ_t was further refined using ARIMA to forecast the behavior of the parameters, ensuring robust and accurate modeling of the dependencies between the climatic factors and dengue transmission.

Next, the selected univariate distributions for the random variables X (e.g., R_{eff}) and Y (e.g., precipitation or temperature) are incorporated into the time-varying copula using Sklar's theorem, yielding a time-varying bivariate distribution function. This construction allows for the derivation of conditional probabilities, which determine the probability of one variable given a fixed value of the other. For instance, the conditional probability $P(X \leq x|Y = y; \theta_t)$ was computed to provide insight into how changes in one climatic factor (such as increased precipitation) affected the transmission of dengue. The final step is to interpret the graph of the conditional probability $P(X \leq x|Y = y; \theta_t)$. This interpretation provides valuable insights into the relationship between the variables and their dependency structure, facilitating predictions based on conditional probabilities derived from the copula model.

3. Results and Discussion

3.1. **Construction of RLUF copula.** Inspired by extreme value theory, we set $f(x, y) = x^a y^b e^{-c_1 x^m - c_2 y^n}$ with $a, b \in \mathbb{R}$, $c_1, c_2 > 0$, and m, n are not equal to zero. Using some formulae in [14], we are able to compute f_1, f_2 and A as follows

$$f_1(x) = \frac{x^a e^{-c_1 x^m}}{n c_2^{\frac{b+1}{n}}} \gamma\left(\frac{b+1}{n}, c_2\right), \tag{2}$$

$$f_2(y) = \frac{y^b e^{-c_2 y^n}}{m c_1^{\frac{a+1}{m}}} \gamma\left(\frac{a+1}{m}, c_1\right) \tag{3}$$

and

$$A = \frac{1}{m c_1^{\frac{a+1}{m}} n c_2^{\frac{b+1}{n}}} \gamma\left(\frac{a+1}{m}, c_1\right) \gamma\left(\frac{b+1}{n}, c_2\right). \tag{4}$$

Noting the expression of $f^1(x, y)$, then $c(x, y)$ leads to the following function

$$C(u, v) = uv + \theta \left[\frac{\gamma\left(\frac{a+1}{m}, c_1 u^m\right)}{m c_1^{\frac{a+1}{m}}} - \frac{\gamma\left(\frac{a+1}{m}, c_1\right)}{m c_1^{\frac{a+1}{m}}} u\right] \left[\frac{\gamma\left(\frac{b+1}{n}, c_2 v^n\right)}{n c_2^{\frac{b+1}{n}}} - \frac{\gamma\left(\frac{b+1}{n}, c_2\right)}{n c_2^{\frac{b+1}{n}}} v\right]. \tag{5}$$

We claim that C in (5) is an RLUF copula.

Theorem 3.1. *The function C in (5) is RLUF copula for*

$$-\frac{1}{\max\{\alpha\gamma_0, \beta\delta\}} \leq \theta \leq -\frac{1}{\min\{\alpha\delta, \beta\gamma_0\}},$$

where

$$\alpha = -\frac{1}{a+1}\frac{\Gamma\left(\frac{a+1}{m},c_1\right)}{mc_1^m}, \quad \beta = \left(\frac{a}{mc_1}\right)^a e^{-\frac{a}{m}} + a,$$
$$\gamma_0 = -\frac{1}{b+1}\frac{\Gamma\left(\frac{b+1}{n},c_2\right)}{nc_2^n}, \quad \delta = \left(\frac{b}{nc_2}\right)^b e^{-\frac{b}{n}} + \gamma_0,$$

with $a, b \in \mathbb{R}$, $c_1, c_2 > 0$ *and* m, n *are not equal to zero.*

Proof. We apply Theorem 2.1 by letting

$$f_1(u) = \frac{1}{mc_1^{\frac{a+1}{m}}}\left[\gamma\left(\frac{a+1}{m}, c_1u^m\right) - \gamma\left(\frac{a+1}{m}, c_1\right)u\right],$$

and

$$f_2(v) = \frac{1}{nc_2^{\frac{b+1}{n}}}\left[\gamma\left(\frac{b+1}{n}, c_2v^n\right) - \gamma\left(\frac{b+1}{n}, c_2\right)v\right].$$

Then $f_1(0) = f_1(1) = f_2(0) = f_2(1) = 0$. We now compute the admissible range of θ by calculating the extrema of the functions f_1' and f_2' given by

$$f_1'(u) = u^a e^{-c_1u^m} - \frac{\gamma\left(\frac{a+1}{m}, c_1\right)}{mc_1^{\frac{a+1}{m}}},$$

and

$$f_2'(v) = v^b e^{-c_2v^n} - \frac{\gamma\left(\frac{b+1}{n}, c_2\right)}{nc_2^{\frac{b+1}{n}}}.$$

Moreover, we have

$$f_1''(u) = u^a e^{-c_1u^m}\left(a - mc_1u^m\right),$$

and

$$f_2''(v) = v^b e^{-c_2v^n}\left(b - nc_2v^n\right),$$

respectively.

By setting these derivatives to zero, we obtain the critical values: $u = 0, \left(\frac{a}{mc_1}\right)^{\frac{1}{m}}$, and $v = 0, \left(\frac{b}{nc_2}\right)^{\frac{1}{n}}$. Since $u \in [0, 1]$, we have the following intervals: $\left(0, \left(\frac{a}{mc_1}\right)^{\frac{1}{m}}\right)$ and $\left(\left(\frac{a}{mc_1}\right)^{\frac{1}{m}}, 1\right)$. For $\varepsilon > 0$, the test numbers are $\left(\frac{a}{(m+\varepsilon)c_1}\right)^{\frac{1}{m}} \in \left(0, \left(\frac{a}{mc_1}\right)^{\frac{1}{m}}\right)$ and $\left(\frac{a}{(m-\varepsilon)c_1}\right)^{\frac{1}{m}} \in \left(\left(\frac{a}{mc_1}\right)^{\frac{1}{m}}, 1\right)$. We substitute these test numbers to f_1'' to determine the interval the function f_1' is increasing or decreasing.

Observe that

$$f_1''\left(\left(\frac{a}{(m+\varepsilon)c_1}\right)^{\frac{1}{m}}\right) = \left[\frac{a}{(m+\varepsilon)c_1}\right]^{\frac{a-1}{m}} e^{-\frac{a}{m+\varepsilon}}\left(\frac{a\varepsilon}{m+\varepsilon}\right) > 0.$$

Inferring that f_1' is increasing on the interval $\left(0, \left(\frac{a}{mc_1}\right)^{\frac{1}{m}}\right)$.

Similarly,

$$f_1''\left(\left(\frac{a}{(m\varepsilon)c_1}\right)^{\frac{1}{m}}\right) = \left[\frac{a}{(m-\varepsilon)c_1}\right]^{\frac{a-1}{m}} e^{-\frac{a}{m-\varepsilon}}\left(-\frac{a\varepsilon}{m-\varepsilon}\right) < 0,$$

concluding that f_1' is decreasing on the interval $\left(\left(\frac{a}{mc_1}\right)^{\frac{1}{m}}, 1\right)$.

Based on these computations, we deduced that the absolute maximum of f_1' occurs at $u = \left(\frac{a}{mc_1}\right)^{\frac{1}{m}}$ which is

$$f_1'\left(\left(\frac{a}{mc_1}\right)^{\frac{1}{m}}\right) = \left(\frac{a}{mc_1}\right)^{\frac{a}{m}} e^{-\frac{a}{m}} - \frac{\gamma\left(\frac{a+1}{m}, c_1\right)}{m{c_1}^{\frac{a+1}{m}}},$$

leaving the endpoints $u = 0$ and $u = 1$ to be compared for the possible occurrence of the absolute minimum.

Solving for $f_1'(0) = -\frac{\gamma\left(\frac{a+1}{m}, c_1\right)}{m{c_1}^{\frac{a+1}{m}}}$ and $f_1'(1) = e^{-c_1} - \frac{\gamma\left(\frac{a+1}{m}, c_1\right)}{m{c_1}^{\frac{a+1}{m}}}$ implies $f_1'(0) < f_1'(1)$, which means that the absolute minimum occurs at $u = 0$.

Hence,

$$\alpha = \inf\{f_1'(u) : u \in [0,1]\} = f_1'(0) = -\frac{-\gamma\left(\frac{a+1}{m}, c_1\right)}{m{c_1}^{\frac{a+1}{m}}},$$

and

$$\beta = \sup\{f_1'(u) : u \in [0,1]\} = f_1'\left(\left(\frac{a}{mc_1}\right)^{\frac{1}{m}}\right) = \left(\frac{a}{mc_1}\right)^{\frac{a}{m}} e^{-\frac{a}{m}} + \alpha.$$

A similar solution can be followed to obtain

$$\gamma_0 = \inf\{f_2'(v) : v \in [0,1]\} = f_2'(0) = -\frac{\gamma\left(\frac{b+1}{n}, c_2\right)}{m{c_2}^{\frac{b+1}{n}}},$$

and

$$\delta = \sup\{f_2'(v) : v \in [0,1]\} = f_2'\left(\left(\frac{b}{nc_2}\right)^{\frac{1}{n}}\right) = \left(\frac{b}{nc_2}\right)^{\frac{b}{n}} e^{-\frac{b}{n}} + \delta.$$

Therefore, the function C is an RLUF copula. □

3.2. **Dependence Properties of the Derived RLUF Copula.** In this section, we derive the Kendall's tau, Spearman's rho, and tail dependence of RLUF copula.

Theorem 3.2. *Let C be the RLUF copula defined in Theorem 3.1. Then the Kendall's tau associated with C is given by*

$$\tau(C) = \frac{8\theta}{mn{c_1}^{\frac{a+1}{m}}{c_2}^{\frac{b+1}{n}}}\left[\frac{\gamma\left(\frac{a+1}{m}, c_1\right)}{2} - \frac{\gamma\left(\frac{a+2}{m}, c_1\right)}{c_1^{\frac{1}{m}}}\right]\left[\frac{\gamma\left(\frac{b+1}{n}, c_2\right)}{2} - \frac{\gamma\left(\frac{b+2}{n}, c_2\right)}{c_2^{\frac{1}{n}}}\right]. \tag{6}$$

Proof. The Kendall's tau can be derived using the following expression from [34],

$$\tau(C) = 8\theta\int_0^1 f_1(u)du \cdot \int_0^1 f_2(v)dv.$$

We compute

$$\int_0^1 f_1(u)du = \frac{1}{mc_1^{\frac{a+1}{m}}}\left[\int_0^1 \gamma\left(\frac{a+1}{m}, c_1u^m\right)du - \int_0^1 \gamma\left(\frac{a+1}{m}, c_1\right)udu\right]$$
$$= \frac{1}{mc_1^{\frac{a+1}{m}}}\left[\int_0^1 \gamma\left(\frac{a+1}{m}, c_1u^m\right)du - \frac{\gamma\left(\frac{a+1}{m}, c_1\right)}{2}\right].$$

We can solve the integral using integration by parts where we assign the following variables:

$$p = \gamma\left(\frac{a+1}{m}, c_1u^m\right); \qquad dq = du,$$

and

$$dp = (c_1u^m)^{\frac{a+1}{m}} e^{-c_1u^m} \cdot mc_1u^{m-1}du; \qquad q = u.$$

which leads to

$$\int_0^1 \gamma\left(\frac{a+1}{m}, c_1u^m\right)du = uv\left(\frac{a+1}{m}, c_1u^m\right)\Big|_0^1 - \int_0^1 (c_1u^m)^{\frac{a+1}{m}} e^{-c_1u^m} \cdot mc_1u^{m-1}du$$
$$= \gamma\left(\frac{a+1}{m}, c_1\right) - \gamma\left(\frac{a+2}{m}, c_1\right)\frac{1}{c_1^m}$$
$$= \frac{1}{mc_1^{\frac{a+1}{m}}}\left[\frac{\gamma\left(\frac{a+1}{m}, c_1\right)}{2} - \frac{\gamma\left(\frac{a+2}{m}, c_1\right)}{c_1^{\frac{1}{m}}}\right].$$

Likewise

$$\int_0^1 f_2(v)dv = \int_0^1 \frac{1}{nc_2^{\frac{b+1}{n}}}\left[\gamma\left(\frac{b+1}{n}, c_2v^n\right) - \gamma\left(\frac{b+1}{n}, c_2\right)v\right]dv$$
$$= \frac{1}{nc_2^{\frac{b+1}{n}}}\left[\frac{\gamma\left(\frac{b+1}{n}, c_2\right)}{2} - \frac{\gamma\left(\frac{b+2}{n}, c_2\right)}{c_2^{\frac{1}{n}}}\right].$$

Combining the results of the two integrals, we obtain the expression as desired. □

Since $\rho(C) = \frac{3}{2}\tau(C)$, we have the following result.

Corollary 3.2.1. *Let C be the RLUF copula defined in Theorem 3.1. Then the Spearman's rho associated with C is given by*

$$\rho(C) = \frac{12\theta}{mnc_1^{\frac{a+1}{m}}c_2^{\frac{b+1}{n}}}\left[\frac{\gamma\left(\frac{a+1}{m}, c_1\right)}{2} - \frac{\gamma\left(\frac{a+2}{m}, c_1\right)}{c_1^{\frac{1}{m}}}\right]\left[\frac{\gamma\left(\frac{b+1}{n}, c_2\right)}{2} - \frac{\gamma\left(\frac{b+2}{n}, c_2\right)}{c_2^{\frac{1}{n}}}\right].$$

Remark 1. *We notice that RLUF copula does not register an upper and lower tail dependency.*

We calculate the upper tail dependence

$$\lambda_U = \lim_{u\to 1^-} \frac{1-2u+C(u,u)}{1-u}$$

by noting that

$$C(u,u) = u^2 + \frac{\theta}{mnc_1^{\frac{a+1}{m}} c_2^{\frac{b+1}{n}}} \left[\gamma\left(\frac{a+1}{m}, c_1 u^m\right) - \gamma\left(\frac{a+1}{m}, c_1\right) u\right] \left[\gamma\left(\frac{b+1}{n}, c_2 u^n\right) - \gamma\left(\frac{b+1}{n}, c_2\right) u\right]$$

and

$$\frac{dC(u,u)}{du} = 2u + \frac{\theta}{mnc_1^{\frac{a+1}{m}} c_2^{\frac{b+1}{n}}} \left[\gamma\left(\frac{a+1}{m}, c_1 u^m\right) - \gamma\left(\frac{a+1}{m}, c_1\right) u\right]$$
$$\left[(c_2 u^n)^{\frac{b+1}{n}-1} e^{-c_2 u^n} \left(nc_2 u^{n-1}\right) - \gamma\left(\frac{b+1}{n}, c_2\right)\right]$$
$$+ \left[\gamma\left(\frac{b+1}{n}, c_2 u^n\right) - \gamma\left(\frac{b+1}{n}, c_2\right) u\right] \left[(c_1 u^m)^{\frac{a+1}{m}-1} e^{-c_1 u^m} \left(mc_1 u^{m-1}\right) - \gamma\left(\frac{a+1}{m}, c_1\right)\right],$$

which leads to

$$\lambda_U = \lim_{u \to 1^-} \frac{-2 + \frac{dC(u,u)}{du}}{-1} = \lim_{u \to 1^-} \frac{-2+2}{-1} = 0.$$

This is similar to the lower tail dependence

$$\lambda_L = \lim_{u \to 0^+} \frac{C(u,u)}{u} = 0.$$

Although the RLUF copula demonstrates superior performance in capturing the non-linear dependencies between R_{eff} and climatic variables, as we will see in the next sections, the RLUF copula does not exhibit tail dependence, as both the upper and lower tail dependence coefficients (λ_U and λ_L) are zero. This suggests that the model is less sensitive to extreme values of temperature and precipitation, which may coincide with severe Dengue outbreaks. Future research could explore copula modifications that incorporate tail dependence for improvement.

3.3. **Probabilistic Modeling with Dengue R_{eff}.** We analyzed the relationship between Dengue's effective reproductive number (R_{eff}), precipitation, and temperature in the Caraga Region. Table 1 provides the descriptive statistics of these variables from January 2015 to December 2020.

Table 1. Descriptive Statistic of the Dengue R_{eff}, Precipitation and Temperature in Caraga Region January 2015 to December 2020

Variables	**Mean**	**SD**	**Minimum**	**Maximum**	**Skewness**	**Kurtosis**
R_{eff}	0.964	0.357	0.00	1.95	-0.381	0.0889
Precipitation	7.223	9.521	0.00	114.99	4.223	30.7571
Temperature	24.068	0.82	20.5	27.15	-0.309	0.4553

The mean R_{eff} of 0.964 indicates moderate disease transmission, with values ranging from 0 to 1.95. Precipitation data exhibits high variability with frequent extreme events, while temperature data shows stability, averaging 24.07°C. Precipitation has a high skewness (4.223), suggesting infrequent but intense rainfall, while the temperature and R_{eff} distributions are relatively symmetric.

Next, we fit the distribution of the three underlying variables to theoretical distributions. Two tests were used for each distribution: (1) the Chi-Square Goodness of Fit test and; (2) the least MSE, AIC and BIC.

TABLE 2. Comparison of Fitted Probability Distribution to R_{eff} of Dengue Disease in Caraga Region at a 95% Confidence Level ($\alpha = 0.05$)

Distributions	Parameters	p-value	Conclusion	MSE	AIC	BIC
3-parameter Dagum	$\alpha = 11.442$ $\beta = 1.336$ $k = 0.20992$	1.00	Accept H_0	0.0165	-3890.64	-8967.69
3-parameter Gamma	$\alpha = 0.34706$ $\beta = 1.39188$ $k = 6.72888$	1.00	Accept H_0	0.00017	-8458.16	-19466.38
3-parameter Logistic	$\mu = 0.98901$ $\sigma = 0.19822$ $k = -0.07808$	1.00	Accept H_0	0.00013	-8458.16	-19466.38

Table 2 compares the fit of three probability distributions (Dagum, Gamma, Logistic) to the Dengue R_{eff} data in the Caraga Region. All distributions passed the chi-square goodness-of-fit test with a p-value of 1.00, indicating that the null hypothesis (H_0) was not rejected. Among the distributions, the 3-parameter Logistic model exhibited the best fit with the lowest Mean Squared Error (MSE = 0.00013), and the lowest Akaike Information Criterion (AIC = -8458.16) and Bayesian Information Criterion (BIC = -19466.38). The 3-parameter Gamma model followed closely in terms of fit, with a slightly higher MSE (0.00017). The Dagum distribution, while still acceptable, showed a relatively higher MSE (0.0165) and thus a weaker fit compared to the other two models.

Figures 1A and 1B visually confirm the strong fit of the 3-parameter Logistic distribution, as both the CDF and PDF curves align well with the empirical data.

Table 3 compares the fit of three probability distributions (General Pareto, Pearson 6, Burr) to the precipitation data in the Caraga Region. All distributions passed the chi-square goodness-of-fit test with a p-value of 1.00, meaning the null hypothesis (H_0) was not rejected.

The 3-parameter General Pareto distribution provided the best fit, as indicated by the lowest Mean Squared Error (MSE = 0.00003), Akaike Information Criterion (AIC = -9825.86), and Bayesian Information Criterion (BIC = -22615.63). The Burr distribution also performed well with a low MSE (0.00004), although it exhibited slightly higher AIC and BIC values. In contrast, the 3-parameter Pearson 6 distribution showed a weaker fit with the highest MSE (0.2188) and significantly higher AIC (-1439.94) and BIC (-3306.33) values compared to the other two distributions. Figures 1C and 1D visually confirm its fit.

TABLE 3. Comparison of Fitted Probability Distribution to Precipitation in Caraga Region at a 95% Confidence Level ($\alpha = 0.05$)

Distributions	Parameters	Chi-Square Test		MSE	AIC	BIC
		p-value	Conclusion			
3-parameter General Pareto	$\mu = -10965$ $\sigma = 5.8902$ $k = 0.1969$	1.00	Accept H_0	0.00003	-9825.86	-22615.63
3-parameter Pearson 6	$\alpha_1 = 1.848$ $\alpha_2 = 5.9111$ $\beta = 39.161$	1.00	Accept H_0	0.2188	-1439.94	-3306.33
Burr	$\alpha = 0.937$ $\beta = 49617$ $k = 7.305$	1.00	Accept H_0	0.00004	-9518.18	-21907.15

TABLE 4. Comparison of Fitted Probability Distribution to Temperature in Caraga Region at a 95% Confidence Level ($\alpha = 0.05$)

Distributions	Parameters	Chi-Square Test		MSE	AIC	BIC
		p-value	Conclusion			
Burr	$\alpha = 43.433$ $\beta = 24.612$ $k = 2.0011$	1.00	Accept H_0	0.00003	-9639.58	-22186.69
Dagum	$\alpha = 15.247$ $\beta = 5.0332$ $g = 19.625$ $k = 0.37395$	1.00	Accept H_0	0.00009	-8803.10	-20257.55
Kumaraswamy	$\alpha_1 = 5.4811$ $\alpha_2 = 283.10$ $a = 20.093$ $b = 32.107$	1.00	Accept H_0	0.00011	-8661.51	-19931.51

Table 4 indicates that all three distributions (Burr, Dagum, and Kumaraswamy) provide a satisfactory fit to the temperature data, as evidenced by the p-value of 1.00 for the Chi-Square Test, which leads to the acceptance of the null hypothesis H_0. Among the distributions, the Burr distribution had the lowest Mean Squared Error (MSE) and Bayesian Information Criterion (BIC), suggesting that it might provide the best fit to the data. The AIC values further support the good fit of these distributions, with lower AIC values indicating better fit. Figures 1E and 1F also confirm the fit.

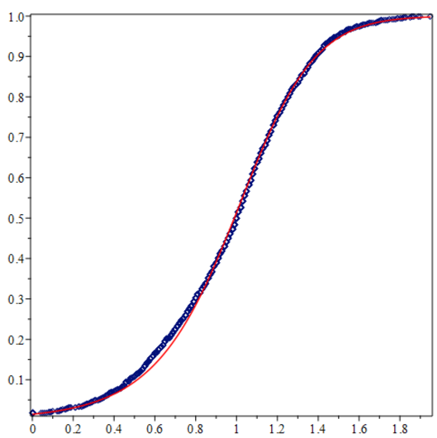

(A) 3-parameter Logistic CDF Fitted to R_{eff}

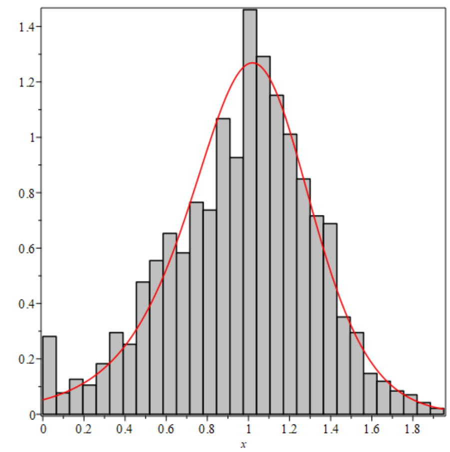

(B) 3-parameter Logistic PDF Fitted to R_{eff}

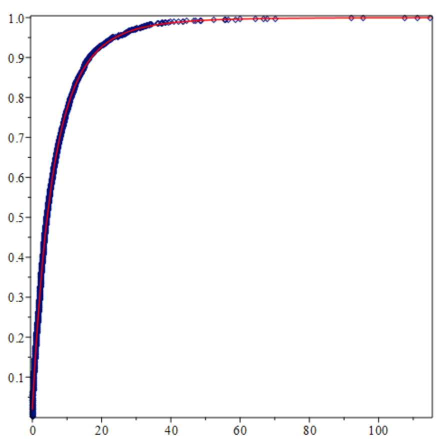

(C) 3-parameter General Pareto CDF Fitted to Precipitation

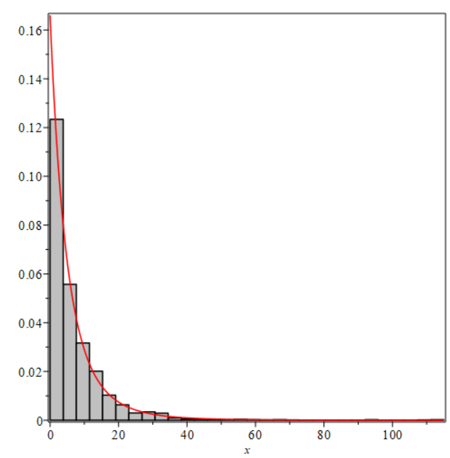

(D) 3-parameter General Pareto PDF Fitted to Precipitation

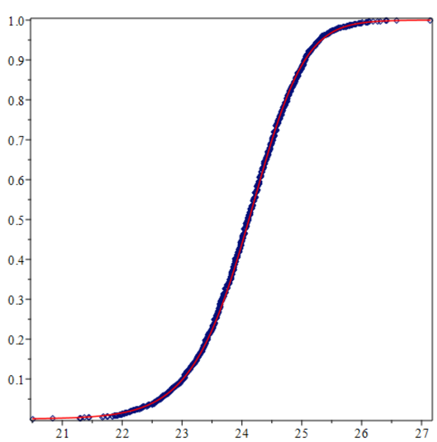

(E) Burr CDF Fitted to Temperature

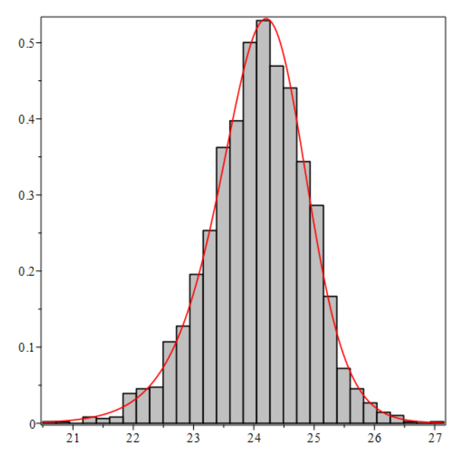

(F) Burr PDF Fitted to Temperature

FIGURE 1. Comparison of CDF and PDF Fits for Different Distributions in the Caraga Region

Table 5. Model Comparison of the Distribution of Effective Reproductive Number and Precipitation in Caraga Region at a 95% Confidence Level ($\alpha = 0.05$)

Copula	Parameters	p-value	Conclusion	MSE	AIC	BIC
Clayton	$\theta = 0.055$	1.00	Accept H_0	0.00001128	-10838.18	-24952.75
AMH	$\theta = 0.101$	1.00	Accept H_0	0.000015	-10552.53	-24295.03
Frank	$\theta = -0.00099$	1.00	Accept H_0	0.037	-3127.49	-7198.24
Gumbel	$\theta = 1.00$	1.00	Accept H_0	0.058	-2703.39	-6221.70
Joe	$\theta = 1.029$	1.00	Accept H_0	0.00002	-10269.57	-23643.47
FGM	$\theta = 0.102$	1.00	Accept H_0	0.00001	-10542.09	-24270.98
RLUF	$a = 0.122$ $b = -0.725$ $c_1 = 2.657$ $c_2 = 4.704$ $m = 0.409$ $n = 1.100$ $\theta = 0.1774$	1.00	Accept H_0	8.62×10^{-6}	-11081.26	-25493.94

Table 5 indicates that all copula models tested had p-values of 1.00 in the Chi-Square Goodness of Fit test, leading to the acceptance of the null hypothesis (H_0) that the sample was drawn from the specified copula. This acceptance suggests that the sample data for the distribution of the effective reproductive number and precipitation fit well with all tested copula models. However, further analysis based on the MSE, AIC, and BIC values can provide insights into the relative goodness of fit among the copula models. Among the tested copula models, the RLUF copula had the smallest MSE, AIC, and BIC, indicating that the RLUF copula is the most suitable copula for describing the simultaneous occurrence of R_{eff} and precipitation.

TABLE 6. Model Comparison of the Distribution of Effective Reproductive Number and Temperature in Caraga Region at a 95% Confidence Level ($\alpha = 0.05$)

Copula	Parameters	p-value	Conclusion	MSE	AIC	BIC
Clayton	$\theta = 0.0682$	1.00	Accept H_0	9.75×10^{-6}	-10976.40	-25271.01
AMH	$\theta = 0.137$	1.00	Accept H_0	0.000011	-10838.45	-24953.37
Frank	$\theta = -0.0009$	1.00	Accept H_0	0.038	-3107.34	-7151.83
Gumbel	$\theta = 1.000$	1.00	Accept H_0	0.057	-2713.36	-6244.67
Joe	$\theta = 1.045$	1.00	Accept H_0	0.000018	-10362.67	-23857.85
FGM	$\theta = 0.140$	1.00	Accept H_0	0.000011	-10818.58	-24907.61
RLUF	$a = 0.063$ $b = -0.570$ $c_1 = 1.014$ $c_2 = 1.014$ $m = 0.989$ $n = 0.950$ $\theta = 0.223$	1.00	Accept H_0	7.40×10^{-6}	-11226.63	-25828.66

Similarly, Table 6 shows the RLUF copula's superior predictive performance compared with the traditional copulas considered. This implies that the RLUF copula better captures the nonlinear dependencies between dengue's R_{eff} and climatic variables, thus offering a more accurate model for understanding and predicting the relationship between climate conditions and dengue transmission.

According to Sklar's theorem, the bivariate distribution of simultaneous occurrence of R_{eff} and precipitation is

$$F_1(x,y) = \frac{1 - \frac{1}{(1+0.3e-y)^5}}{1+(1.4-0.4x)^{12.5}} + 0.02\left[1.6 - \Gamma\left(2.7, 2.7\left(\frac{1}{1+(1.4-0.4x)^{12.5}}\right)^{0.41}\right) - \frac{0.9}{1+(1.4-0.4x)^{12.8}}\right] \left[0.002 - 2 - \Gamma\left(0.2, 4.7\left(1 - \frac{1}{(1+0.3y)^{5.1}}\right)^{1.1}\right) + \frac{3.6}{(1+0.03y)^{5.1}}\right] \tag{7}$$

and the bivariate distribution of simultaneous occurrence of R_{eff} and temperature is

$$F_2(x,y) = \frac{1 - \frac{1}{(1+3.8\times 10^{-61}y^{43.4})^2}}{1+(1.4-0.4x)^{12.8}} + 0.2\left[1 - \Gamma\left(1.1, 1.01\left(\frac{1}{1+(1.4-0.4x)^{12.8}}\right)^{0.99}\right) - \frac{0.6}{1+(1.4-0.4x)^{12.8}}\right] \left[0.3 - \Gamma\left(0.5, 1.01\left(1 - \frac{1}{(1+3.8\times 10^{-61}y^{43.4})^2}\right)^{0.95}\right) + \frac{1.7}{(1+3.8\times 10^{-61}y^{43.4})^2}\right]. \tag{8}$$

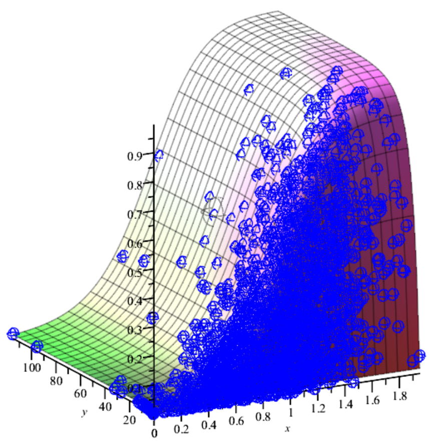

(A) Bivariate Logistic-General Pareto Fitted to Simultaneous Occurrence of R_{eff} and Precipitation

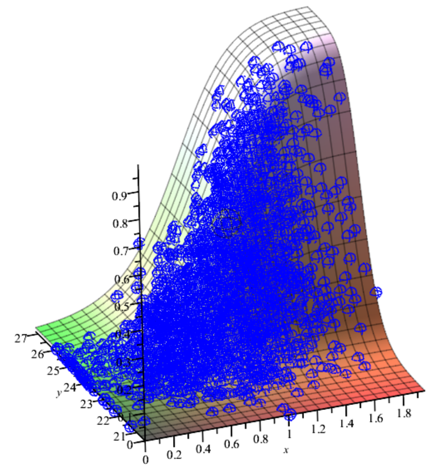

(B) Bivariate Logistic-Burr Fitted to Simultaneous Occurrence of R_{eff} and temperature

FIGURE 2. Bivariate Distributions of Simultaneous Occurrence of R_{eff} and Precipitation, and R_{eff} and Temperature

In the subsequent section, we introduce the time-varying RLUF copula, which provides an additional layer of accuracy by dynamically adjusting dependency parameters over time. The rolling time window approach, combined with ARIMA forecasting, allows the model to reflect real-time changes in climatic conditions and their impact on dengue transmission. This dynamic modeling marks a substantial advancement over static copula models, which cannot account for the evolving dependencies.

First, we generate a sequence of values of the copula parameter θ of the RLUF copula using the rolling window approach with a length of 100 data points per window. We fit 100 data points to the RLUF copula holding the parameters a, b, c_1, c_2, m and n and estimate the copula parameter, then traverse one data point while maintaining the length of the window.

Next, we modeled the sequence of the generated copula parameter values using the ARIMA process. Figures 3A and 3B present the time series plot of the copula parameter θ_t for the bivariate distribution of R_{eff} and precipitation and bivariate distribution of R_{eff} and temperature, respectively, based on RLUF copula while holding other parameters constant.

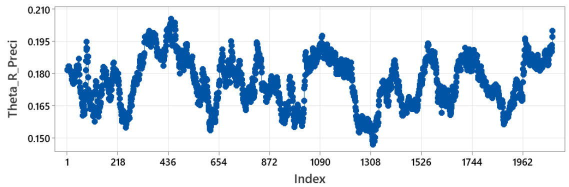

(A) Time Series Plot of the Estimated Copula Parameter θ_t for R_{eff} and Precipitation

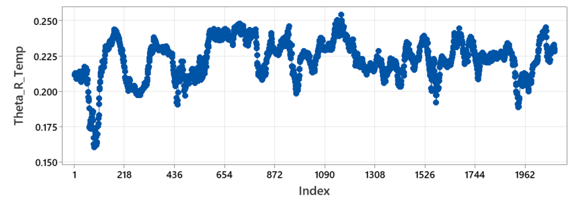

(B) Time Series Plot of the Estimated Copula Parameter θ_t for R_{eff} and Temperature

FIGURE 3. Time Series Plots of the Estimated Copula Parameter θ

Tables 7 and 8 provide the Augmented-Dicky-Fuller (ADF) test for the copula parameter θ_t for the distribution of R_{eff} and precipitation, and the distribution of R_{eff} and temperature, respectively, at a 95% confidence level $(\alpha = 0.05)$. The result shows that the distributions' copula parameter θ_t should first undergo differencing $(d = 1)$ to satisfy the stationary assumption.

TABLE 7. Augmented Dickey-Fuller Test for Estimated Copula Parameter θ_t for R_{eff} and Precipitation at a 95% Confidence Level $(\alpha = 0.05)$

Differencing	**Test Statistic**	**Critical Value** $(\alpha = 0.05)$	p**-value**	**Conclusion**
0	-3.17846	-3.41259	0.089	Accept H_0
1	-4.17525	-3.41259	0.005	Reject H_0

TABLE 8. Augmented Dickey-Fuller Test for Estimated Copula Parameter θ_t for R_{eff} and Temperature at a 95% Confidence Level $(\alpha = 0.05)$

Differencing	**Test Statistic**	**Critical Value** $(\alpha = \mathbf{0.05})$	**p-value**	**Conclusion**
0	-3.25114	-3.41259	0.075	Accept H_0
1	-3.88913	-3.41259	0.013	Reject H_0

From Table 9, the best ARIMA model for the time series of the estimated copula parameter θ_t for the distribution of R_{eff} and precipitation is $ARIMA(1,1,2)$ because it has the lowest values of AIC and BIC.

TABLE 9. Comparison of the Possible ARIMA Models for the Time Series of Estimated Copula Parameter θ_t for R_{eff} and Precipitation with $I = 1$

p	**q**	**Loglikelihood**	**AIC**	**BIC**
1	1	10394	-20780	-20757
1	2	10394.4	-20778.9	-20750.6

Similarly, Table 10 provides evidence that the best time-series model for describing the behavior of the estimated copula parameter θ_t for the distribution of R_{eff} and temperature is $ARIMA(1,1,1)$.

TABLE 10. Comparison of the Possible ARIMA Models for the Time Series of Estimated Copula Parameter θ_t for R_{eff} and Temperature with $I = 1$

p	**q**	**Loglikelihood**	**AIC**	**BIC**
1	1	10079.5	-20151	-20128.4
1	2	10079.8	-20149.6	-20121.4
1	3	10080.2	-20148.4	-20114.5

From Table 11, the equation used to forecast θ_t for the distribution of R_{eff} and precipitation based on RLUF copula will be

$$\theta_t = 0.3495\theta_{t-1} + \varepsilon_t + 0.124\varepsilon_{t-1} + 6 \times 10^{-6} \quad (9)$$

where ε_t and ε_{t-1} are the errors.

Table 11. Final Estimates of the Parameters of ARIMA Models for the Time Series of Estimated Copula Parameter θ_t for R_{eff} and Precipitation with $I = 1$

Process	**Coefficients**	**SE**	**t-value**	**p-value**
AR(1)	0.3495	0.0875	3.99	0.00
MA(1)	0.1249	0.0927	1.35	0.178
Constant	6×10^{-6}	3.2×10^{-4}	0.19	0.853

Likewise, based on the final estimates of the parameters of ARIMA models presented in Table 12, the equation used to forecast θ_t for the distribution of R_{eff} and temperature based on RLUF copula will be

$$\theta_t = 0.5474\theta_{t-1} + \varepsilon_t + 0.387\varepsilon_{t-1} + 4 \times 10^{-6} \tag{10}$$

where ε_t and ε_{t-1} are the errors.

Table 12. Final Estimates of the Parameters of ARIMA Models for the Time Series of Estimated Copula Parameter θ_t for R_{eff} and Temperature with $I = 1$

Process	**Coefficients**	**SE**	**t-value**	**p-value**
AR(1)	0.5474	0.0902	6.07	0.00
MA(1)	0.3870	0.0994	3.89	0.00
Constant	4×10^{-6}	2.6×10^{-5}	0.16	0.872

Tables 13 and 14 shows the superiority of the time-varying RLUF copula over RLUF in modeling the distribution of R_{eff} and precipitation with fixed parameters $(a = 0.122, b = -0.725, c_1 = 2.657, c_2 = 4.704, m = 0.409$ and $n = 1.1)$, and the distribution of R_{eff} and temperature with fixed parameters $(a = 0.063, b = -0.57, c_1 = 1.014, c_2 = 1.014, m = 0.989$ and $n = 0.95)$.

Table 13. Model Comparison of the Distribution of Effective Reproductive Number and Precipitation with Fixed Parameters $(a = 0.122, b = -0.725, c_1 = 2.657, c_2 = 4.704, m = 0.409$ and $n = 1.100)$

Copula	**Chi-Square Goodness of Fit Test**		**MSE**	**AIC**	**BIC**
	p-values	**Conclusion**			
RLUF	1.00	Accept H_0	8.63×10^{-6}	-11081.27	-25493.95
Time-varying RLUF	1.00	Accept H_0	8.57×10^{-6}	-11090.15	-25517.5

Table 14. Model Comparison of the Distribution of Effective Reproductive Number and Temperature with Fixed Parameters $(a = 0.063, b = -0.570, c_1 = 1.014, c_2 = 1.014, m = 0.989$ and $n = 950)$

Copula	**Chi-Square Goodness of Fit Test**		**MSE**	**AIC**	**BIC**
	p-values	**Conclusion**			
RLUF	1.00	Accept H_0	7.41×10^{-6}	-11226.63	-25828.67
Time-varying RLUF	1.00	Accept H_0	7.35×10^{-6}	-11235.36	-25851.85

3.4. **Time-varying Conditional Distribution.** We will now apply the concept of conditional distribution to determine the behavior of dengue spread as the temperature or precipitation increases at a specific time.

Given the events A and B, the probability of occurrence of A given B is given by

$$P(A|B) = \frac{P(A \cap B)}{P(B)}.$$

If the event A is the event that the spread of Dengue disease is decreasing $(X \leq 1)$ and B is the event that the precipitation is equal to y $(Y = y)$, where X and Y are random variables associated with R_{eff} and precipitation, respectively. Then

$$\begin{aligned} P(X \leq 1|Y = y) &= \frac{P(X \leq 1 \cap Y = y)}{P(Y = y)} \\ &= \frac{\frac{\partial}{\partial y} F_1(x, y)}{\frac{d}{dy} F_P(y)}, \end{aligned}$$

where F_1 is the bivariate distribution of R_{eff} and precipitation, while F_P is the CDF of precipitation. If we are about to consider the specific time these events will occur, then we have

$$P(X \leq x|Y = y) = \frac{\frac{\partial}{\partial y} F_1(x, y; \theta_t)}{\frac{d}{dy} F_p(y)}.$$

Likewise, the chance that the Dengue disease will decrease $(X \leq 1)$ given a specific temperature $(Z = z)$ at a specific time, is

$$P(X \leq 1|Y = y) = \frac{\frac{\partial}{\partial z} F_2(x, z; \theta_t)}{\frac{d}{dy} F_T(y)},$$

where F_2 is the time bivariate distribution of R_{eff} and temperature, while F_T is the CDF of temperature.

Figures 4A and 4B present graphs of $P(R_{\text{eff}} \leq 1|\text{Precipitation} = y; \theta_t)$ and $P(R_{\text{eff}} \leq 1|\text{Temperature} = z; \theta_t)$, respectively, for $t = 1, 160, 175, 304$ and 360 days. Based on Figure 4A, the chance of a decrease in the dengue spread decreases as precipitation increases. In other words, the risk of dengue increases with increasing precipitation. Our study results were supported by [24], who found that the risk of dengue increases between 0-3 months after extremely wet conditions. On the other hand, Figure 4B shows that as the temperature increases to $22.6°C$, the chance of a decrease in dengue spread increases, but the risks of dengue are high between $22.6°C$ and $24.5°C$. The chance of being safe from dengue spikes up to 24.5 $°C$. It was highlighted in [12] that there is a specific range of temperatures in which dengue risk is high, but very high temperatures may reduce the risk of infection.

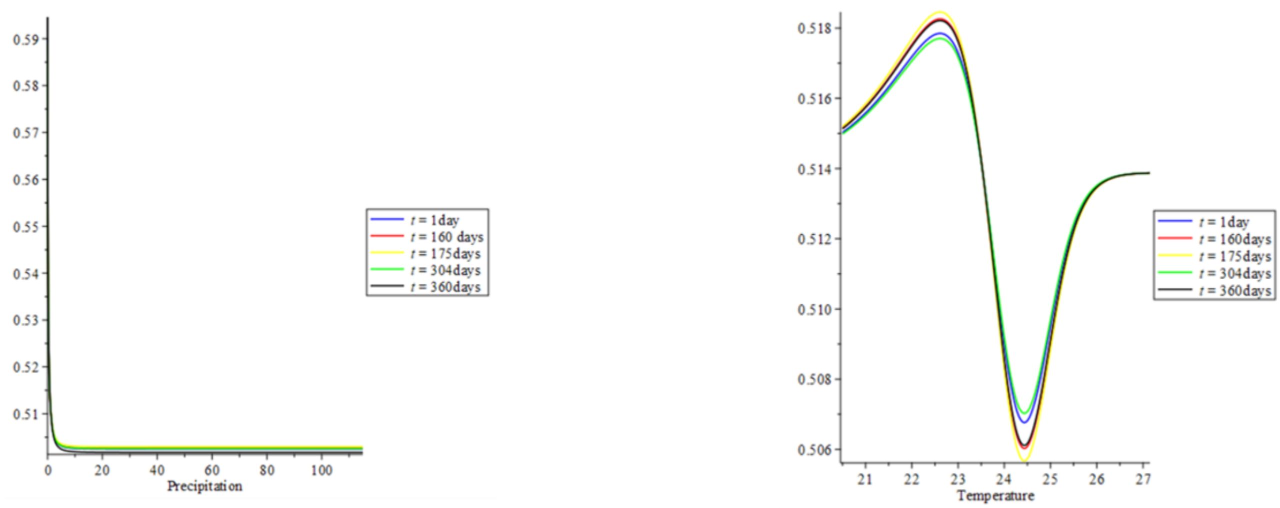

(A) $P(R_{\text{eff}} \leq 1|\text{Precipitation} = y; \theta_t)$

(B) $P(R_{\text{eff}} \leq 1|\text{Temperature} = z; \theta_t)$

FIGURE 4. Behavior of Probability of Decrease in Dengue Spread, R_{eff} Through Time as Precipitation and Temperature Increases

4. Conclusion

This study developed a novel RLUF-type copula using the Rüschendorf method to model the time-varying dependencies between climatic factors (precipitation, temperature) and Dengue's Effective Reproductive Number (R_{eff}). The RLUF-type copula demonstrated superior predictive performance compared to traditional copulas such as Clayton, Gumbel, and Frank, as evidenced by lower MSE, AIC, and BIC values. By incorporating time-varying copulas with rolling window estimation and ARIMA modeling, this study successfully captured dynamic shifts in dependencies over time, providing robust forecasting capabilities for Dengue transmission based on changing climatic conditions.

The results offer a deeper understanding of the complex, nonlinear relationships between temperature, precipitation, and Dengue outbreaks, showing that higher precipitation generally increases transmission risk, while temperature effects fluctuate within critical thresholds. The practical application of these findings can significantly improve early-warning systems and support more effective intervention strategies in regions like the Caraga Region of the Philippines, where Dengue remains a persistent threat.

While the RLUF copula captures the dependencies between Dengue transmission and climatic factors, the absence of tail dependence presents an opportunity for further improvement. Future research should focus on enhancing the copula to incorporate tail dependence, which would allow for a more robust modeling of extreme climatic events and their potential to trigger large-scale outbreaks. Such enhancements would offer a more comprehensive framework for public health forecasting and intervention strategies.

This versatile framework not only improves public health forecasting for Dengue but also offers a foundation for predictive models of other climate-sensitive diseases across various geographic regions, making it a powerful tool for global public health risk assessment and intervention strategies. This study sets a new benchmark for dynamic epidemiological models, providing essential tools to address the increasing challenges posed by climate change and global public health risks.

Acknowledgements

The authors would like to thank the Department of Health of the Caraga Region for providing essential data on daily dengue cases. We also extend our gratitude to Juni Wijayanti Puspita of Institut Teknologi Bandung for generating the R_{eff} using their model.

Authors' Contributions

JP Arcede and MO Macalos conceptualized and designed the study. JVB Deluao collected and curated the data, and contributed to the interpretation of the results. JVB Deluao and MO Macalos assisted in the development of the model and drafted the manuscript. JVB Deluao provided the theoretical proofs, while MO Macalos coded the model script. All authors reviewed and approved the final version of the manuscript.

Conflicts of Interest

The authors declare that there are no conflicts of interest regarding the publication of this paper.

References

[1] Department of Health (CCHD), Dengue rising with rain; Mosquitos to blame, DOH Press Release, July 2024.

[2] J.P. Arcede, R.N. Paluga, M.O. Macalos, N. Sharif, Construction of Sarmanov-type copulae through Rüschendorf method, in: F. Yosuf, S. Jamaludin (Eds.), Copula Modeling and its Applications, Penerbit UTM Press, Malaysia, 2023.

[3] N. Bezak, K. Zabret, M. Šraj, Application of copula functions for rainfall interception modelling, Water 10 (2018), 995. https://doi.org/10.3390/w10080995.

[4] M.I. Bhatti, H.Q. Do, Recent development in copula and its applications to the energy, forestry and environmental sciences, Int. J. Hydrogen Energy 44 (2019), 19453–19473. https://doi.org/10.1016/j.ijhydene.2019.06.015.

[5] M. Chan, M.A. Johansson, The incubation periods of dengue viruses, PLoS ONE 7 (2012), e50972. https://doi.org/10.1371/journal.pone.0050972.

[6] J. Cheng, H. Bambrick, L. Yakob, G. Devine, F.D. Frentiu, G. Williams, Z. Li, W. Yang, W. Hu, Extreme weather conditions and dengue outbreak in guangdong, china: spatial heterogeneity based on climate variability, Environ. Res. 196 (2021), 110900. https://doi.org/10.1016/j.envres.2021.110900.

[7] G. De Luca, G. Rivieccio, Modeling and simulating rainfall and temperature using rotated bivariate copulas, Hydrology 10 (2023), 236. https://doi.org/10.3390/hydrology10120236.

[8] C. Depradine, E. Lovell, Climatological variables and the incidence of dengue fever in barbados, Int. J. Environ. Health Res. 14 (2004), 429–441. https://doi.org/10.1080/09603120400012868.

[9] A. Dias, P. Embrechts, Modeling exchange rate dependence dynamics at different time horizons, J. Int. Money Finance 29 (2010), 1687–1705. https://doi.org/10.1016/j.jimonfin.2010.06.004.

[10] F. Durante, C. Sempi, Principles of copula theory, Chapman and Hall/CRC, 2015. https://doi.org/10.1201/b18674.

[11] N.C. Dzupire, P. Ngare, L. Odongo, A copula based bi-variate model for temperature and rainfall processes, Sci. Afr. 8 (2020), e00365. https://doi.org/10.1016/j.sciaf.2020.e00365.

[12] J. Fan, W. Wei, Z. Bai, C. Fan, S. Li, Q. Liu, K. Yang, A systematic review and meta-analysis of dengue risk with temperature change, Int. J. Environ. Res. Public Health 12 (2014), 1–15. https://doi.org/10.3390/ijerph120100001.

[13] M. Fischer, C. Köck, S. Schlüter, F. Weigert, An empirical analysis of multivariate copula models, Quant. Finance 9 (2009), 839–854. https://doi.org/10.1080/14697680802595650.

[14] I.S. Gradshteĭn, I.M. Ryzhik, A. Jeffrey, Table of integrals, series, and products, Academic Press, Amsterdam, 2009.

[15] P. Guo, T. Liu, Q. Zhang, L. Wang, J. Xiao, Q. Zhang, G. Luo, Z. Li, J. He, Y. Zhang, W. Ma, Developing a dengue forecast model using machine learning: a case study in China, PLoS Negl. Trop. Dis. 11 (2017), e0005973. https://doi.org/10.1371/journal.pntd.0005973.

[16] Y.L. Hii, J. Rocklöv, N. Ng, C.S. Tang, F.Y. Pang, R. Sauerborn, Climate variability and increase in intensity and magnitude of dengue incidence in singapore, Glob. Health Action 2 (2009), 2036. https://doi.org/10.3402/gha.v2i0.2036.

[17] B. Hussain, N.A. Qureshi, R.A. Buriro, S.S. Qureshi, A.A. Pirzado, T.A. Saleh, Interdependence between temperature and precipitation: modeling using copula method toward climate protection, Model. Earth Syst. Environ. 8 (2022), 2753–2766. https://doi.org/10.1007/s40808-021-01256-8.

[18] H. Joe, Multivariate models and multivariate dependence concepts, Chapman and Hall/CRC, 1997. https://doi.org/10.1201/9780367803896.

[19] X.Y. Leung, R.M. Islam, M. Adhami, D. Ilic, L. McDonald, S. Palawaththa, B. Diug, S.U. Munshi, M.N. Karim, A systematic review of dengue outbreak prediction models: current scenario and future directions, PLoS Negl. Trop. Dis. 17 (2023), e0010631. https://doi.org/10.1371/journal.pntd.0010631.

[20] A.D. Ligsay., K.J.M. Tambio., M.J.M. Aytona, G.J.D. Alejandro, Z.J.G. Regencia, E.S. Baja and R. Paúl, Assessing Entomological and Epidemiological Efficacy of Pyriproxyfen-Treated Ovitraps in the Reduction of Aedes Species: A Quasi-Experiment on Dengue Infection Using Saliva Samples., *Multidisciplinary Digital Publishing Institute*, 19(5) (2022), 3026–3026. https://doi.org/10.3390/ijerph19053026.

[21] Y. Li, Q. Dou, Y. Lu, H. Xiang, X. Yu, S. Liu, Effects of ambient temperature and precipitation on the risk of dengue fever: a systematic review and updated meta-analysis, Environ. Res. 191 (2020), 110043. https://doi.org/10.1016/j.envres.2020.110043.

[22] R. Lowe, T.C. Bailey, D.B. Stephenson, R.J. Graham, C.A.S. Coelho, M. Sá Carvalho, C. Barcellos, Spatio-temporal modelling of climate-sensitive disease risk: towards an early warning system for dengue in Brazil, Comput. Geosci. 37 (2011), 371–381. https://doi.org/10.1016/j.cageo.2010.01.008.

[23] R. Lowe, A. Gasparrini, C.J. Van Meerbeeck, C.A. Lippi, R. Mahon, A.R. Trotman, L. Rollock, A.Q.J. Hinds, S.J. Ryan, A.M. Stewart-Ibarra, Nonlinear and delayed impacts of climate on dengue risk in barbados: a modelling study, PLOS Med. 15 (2018), e1002613. https://doi.org/10.1371/journal.pmed.1002613.

[24] R. Lowe, S.A. Lee, K.M. O'Reilly, O.J. Brady, L. Bastos, et al. Combined effects of hydrometeorological hazards and urbanisation on dengue risk in Brazil: a spatiotemporal modelling study, Lancet Planet. Health 5 (2021), e209–e219. https://doi.org/10.1016/S2542-5196(20)30292-8.

[25] V.R. Louis, R. Phalkey, O. Horstick, P. Ratanawong, A. Wilder-Smith, Y. Tozan, P. Dambach, Modeling tools for dengue risk mapping - a systematic review, Int. J. Health Geograph. 13 (2014), 50. https://doi.org/10.1186/1476-072X-13-50.

[26] P.J.W. Mah, M. Shitan, Construction of a new bivariate copula based on Rueschendorf method, Appl. Math. Sci. 8 (2014), 7645–7658. https://doi.org/10.12988/ams.2014.48644.

[27] M.T. Montemayor, DOH: Dengue cases 15% higher in 2024 1H. https://www.pna.gov.ph/articles/1228003, accessed September 2, 2024.

[28] I. Ismail, F.N.N. Abd Mutalip, K. Jacob, A comprehensive review on the development of copulas in financial field, J. Intell. Fuzzy Syst. 45 (2023), 6047–6062. https://doi.org/10.3233/JIFS-223481.

[29] R.B. Nelsen, An introduction to copulas, Springer, New York, 2006. https://doi.org/10.1007/0-387-28678-0.

[30] N. Nuraini, I.S. Fauzi, M. Fakhruddin, A. Sopaheluwakan, E. Soewono, Climate-based dengue model in semarang, indonesia: predictions and descriptive analysis, Infect. Dis. Model. 6 (2021), 598–611. https://doi.org/10.1016/j.idm.2021.03.005.

[31] Z. Pabaghi, O. Bazrafshan, H. Zamani, M. Shekari, V.P. Singh, Bivariate analysis of extreme precipitation using copula functions in arid and semi-arid regions, Atmosphere 14 (2023), 275. https://doi.org/10.3390/atmos14020275.

[32] P.K. Pandey, L. Das, D. Jhajharia, V. Pandey, Modelling of interdependence between rainfall and temperature using copula, Model. Earth Syst. Environ. 4 (2018), 867–879. https://doi.org/10.1007/s40808-018-0454-9.

[33] J.W. Puspita, M. Fakhruddin, N. Nuraini, E. Soewono, Time-dependent force of infection and effective reproduction ratio in an age-structure dengue transmission model in bandung city, indonesia, Infect. Dis. Model. 7 (2022), 430–447. https://doi.org/10.1016/j.idm.2022.07.001.

[34] J. Rodríguez-Lallena, A new class of bivariate copulas, Stat. Probab. Lett. 66 (2004), 315–325. https://doi.org/10.1016/j.spl.2003.09.010.

[35] A. Rohani, Y.C. Wong, I. Zamre, H.L. Lee, M.N. Zurainee, The effect of extrinsic incubation temperature on development of dengue serotype 2 and 4 viruses in Aedes aegypti (L.), Southeast Asian J. Trop. Med. Public Health, 40 (2009), 942–950.

[36] L. Rüschendorf, Construction of multivariate distributions with given marginals, Ann. Inst. Stat. Math. 37 (1985), 225–233. https://doi.org/10.1007/BF02481093.

[37] S. Sharmin, K. Glass, E. Viennet, D. Harley, Interaction of mean temperature and daily fluctuation influences dengue incidence in dhaka, bangladesh, PLoS Negl. Trop. Dis. 9 (2015), e0003901. https://doi.org/10.1371/journal.pntd.0003901.

[38] X. Wu, L. Lang, W. Ma, T. Song, M. Kang, J. He, Y. Zhang, L. Lu, H. Lin, L. Ling, Non-linear effects of mean temperature and relative humidity on dengue incidence in Guangzhou, China, Sci. Total Environ. 628–629 (2018), 766–771. https://doi.org/10.1016/j.scitotenv.2018.02.136.

[39] J. Xiang, A. Hansen, Q. Liu, X. Liu, M.X. Tong, Y. Sun, S. Cameron, S. Hanson-Easey, G.-S. Han, C. Williams, P. Weinstein, P. Bi, Association between dengue fever incidence and meteorological factors in Guangzhou, China, 2005–2014, Environ. Res. 153 (2017), 17–26. https://doi.org/10.1016/j.envres.2016.11.009.

[40] S. Yin, C. Ren, Y. Shi, J. Hua, H.-Y. Yuan, L.-W. Tian, A systematic review on modeling methods and influential factors for mapping dengue-related risk in urban settings, Int. J. Environ. Res. Public Health 19 (2022), 15265. https://doi.org/10.3390/ijerph192215265.

[41] L. Zhang, V.P. Singh, Bivariate rainfall frequency distributions using archimedean copulas, J. Hydrol. 332 (2007), 93–109. https://doi.org/10.1016/j.jhydrol.2006.06.033.

[42] R.G. Cong, M. Brady, The interdependence between rainfall and temperature: copula analyses, Sci. World J. 2012 (2012), 405675. https://doi.org/10.1100/2012/405675.

[43] M.G. Pizon, R.N. Paluga, N. Rolando, A special case of Rodriguez-Lallena and Ubeda-Flores copula based on Ruschendorf method, Appl. Appl. Math. Int. J. 17 (2022), 18–22.